

Monte Carlo Simulations of Stretched Charged Polymers[†]

Malek O. Khan* and Derek Y. C. Chan

Particulate Fluids Processing Centre, Department of Mathematics & Statistics, The University of Melbourne, Parkville, Victoria 3010, Australia

Received: October 31, 2002; In Final Form: March 25, 2003

The force-extension behavior of charged polymers is investigated by the means of Monte Carlo simulations in the stress ensemble, strain ensemble and by a method which gives the free energy for a chosen range of end-to-end distances. All three methods are equivalent within statistical limits. To focus on the effects of polymer charge on the force-extension curve, we have studied net-neutral polyampholytes as a function of charge block size and polyelectrolytes with neutralizing counterions of various valences. The force-extension curves of polyampholytes with random charge sequences or small charge block sizes or polyelectrolytes with multivalent counterions are similar to force-extension curves for uncharged polymers. Polyampholytes with large charge block sizes can form pearl-necklace structures which give rise to a plateau in the force-extension curve.

1. Introduction

Many naturally occurring polymers and those synthesized for industrial purposes carry ionizable groups. For example, synthetic charged polymers can be found in the medical, food, photographic, cosmetic, and other industries. In nature, DNA, RNA, and proteins are important examples of polymers that bear charges. Polyelectrolytes (PEs) are polymers that carry charges of only one sign, whereas polyampholytes (PAs) refer to polymers with both positive and negative charges.

The theory of the behavior of neutral polymers in dilute solution is well established.^{1,2} Polyelectrolytes have also been studied extensively³ and, although some questions such as the persistence length³ and the behavior of highly charged PEs^{4–6} remain open, a good understanding of PEs have developed. The interest in polyampholytes is more recent and to some extent sparked by their closeness to proteins. Because of the mixture of charges, it is more demanding to study their complex behavior, both experimentally^{7,8} and theoretically.^{9–15}

Experiments facilitating powerful single molecule manipulation have recently been used to extract mechanical information about polymers.^{16–19} In these experiments, an AFM tip or an optical tweezer is used to extend the polymer, and both the length and the applied force are recorded to construct a force-extension curve.

Mechanical stability is important for the function of polymers, and many different molecules have been examined. For example, DNA condensed by multivalent counterions can be described by a wormlike chain (WLC) model.²⁰ Although simple models like the WLC or freely jointed chain (FJC) are readily used to describe many polymer features, some molecules show a much more complicated behavior.

One example is the muscle protein titin, whose force-extension curve has a saw-tooth shape.²¹ When stretching the chain, a certain domain is unfolded, and when that domain is fully stretched, the force is relaxed until another domain starts

to unfold. Unfolding of multiple compact domains leads to the saw-tooth pattern.

Another debated topic is the existence of the Rayleigh instability in single polymer chains. The question is whether under an expanding force, such as a net charge or external field, balanced by a compacting force, such as hydrophobic or electrostatic forces, the polymer can assume a pearl-necklace structure.^{12,22,23} Although this has not been observed directly, it is thought that plateaus in the force-extension curve might reflect the Rayleigh instability.¹⁹ In this paper, we will discuss this phenomenon in the context of charged polymers.

It is not always easy to deduce unambiguously conformation properties from force-extension data. Therefore, it is desirable to undertake model studies of charged polymers to elucidate the generic behavior of such systems. In this work, computer simulation is used as a tool to facilitate understanding of the physical mechanisms involved. Simulation studies have earlier been performed for the stretching of polymers without charges.^{24–27} Focusing on charged polymers, three different ways of simulating stretched polymers are explored here:

(1) A known force is applied and the resulting extension is measured; this is called a stress ensemble.

(2) A certain extension is given and the resulting force is measured; this is referred to as a strain ensemble.

(3) A method in which the potential of mean force is calculated in one simulation for a certain range of the extension. Differentiating the potential of mean force gives the force-extension curve.

For the charged polymers systems studied here, all three approaches produce the same results within the statistical uncertainties, and can be used interchangeably.

Also, in an attempt to model different experimental setups, the effects of attaching the polymer ends to zero, one, and two walls have been investigated. It is shown that the influence of the walls are of negligible importance at all but the smallest extensions, for which restrictions on the conformational freedom imposed by the walls become significant.

In section 2, the system and its Hamiltonian are presented and the three simulation approaches outlined above are described

[†] Part of the special issue "International Symposium on Polyelectrolytes".

* To whom correspondence should be addressed. E-mail: m.khan@ms.unimelb.edu.au.

in detail. As a reference system, force-extension results are shown for neutral polymers in section 3. Three different stretching regimes are observed: entropic stretching where monomers are rearranged while the bond length is kept constant; enthalpic stretching where the individual bonds are stretched; and the finite extensibility regime where the monomers are ordered in the direction of the applied force and the bonds cannot be stretched further resulting in a steep increase in the force for further stretching. In section 4, we consider the behavior of stretched polyampholytes and show that for block-polyampholytes increasing block size leads to a bigger contractive force which resists the external stretching. For these polyampholytes, there is a plateau in the force-extension curve which coincides with the regime of pearl-necklace formation in the polymer conformation. Random polyampholytes do not adopt the pearl-necklace structures because the average block size is too small. In section 5, polyelectrolytes are discussed. For the case with monovalent counterions, the PE is already stretched and only the finite extensibility regime is explored. For higher valence counterions, the PE contracts, but only to about the size of an uncharged chain, and the stretching behavior closely follows that of the uncharged chain.

To focus on the effects of electrostatic interactions associated with the polymer, we have not studied the effect of any added salt. Thus, only net neutral polyampholytes and polyelectrolytes with neutralizing counterions are considered.

2. The Model and Simulation Methods

In this section, the model of the charged polymer systems is first described followed by the three different methods for simulating extended polymers.

2.1. Model of an Undisturbed Polymer. The basic system consists of a single polymer with a total number of monomers N , which is modeled as a chain of hard sphere monomers with diameter d . Each monomer is connected to its neighbor by either harmonic springs with force constant K or a rigid but freely rotating bond of fixed length b . All simulations are carried out in the so-called primitive model whereby the solvent is described by the dielectric constant ϵ_r .

When studying polyelectrolytes, the polymer is enclosed in a cell together with its counterions, with N_c being the number of neutralizing counterions. The effects of added salt is left to a future study. See section 2.2 for more details of the cell model. Polyelectrolytes are only studied within the stress ensemble. All three methods could have been used to study PEs, but because it is time-consuming due to the included counterions, only one method is used. For the polyampholytes, there are no counterions because only net-neutral PAs are considered. PAs and uncharged polymers are studied with all three methods.

The Hamiltonian for the undisturbed system, in the absence of an external force, is given by

$$U_0 = U_{\text{bond}} + U_{\text{el}} + U_{\text{hc}} \quad (1)$$

where

$$U_{\text{bond}} = \frac{1}{2} \sum_{i=1}^{N-1} K |\mathbf{r}_i - \mathbf{r}_{i+1}|^2 \quad (2)$$

is the contribution due to the harmonic springs joining neighboring monomers and $|\mathbf{r}_i - \mathbf{r}_{i+1}|$ is the distance between consecutive monomers. For the case of bonds with fixed lengths, U_{bond} in eq 1 will be replaced by the constraint of a freely rotating bond

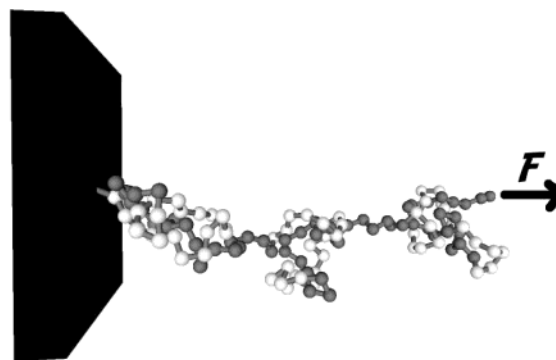


Figure 1. Schematic figure of the model, with one wall, used in the stress ensemble. All particles are enclosed by the wall and an outer sphere (not shown) resulting in a cell with the shape of a hemisphere. The different charges are distinguished by the two shades of gray and the polymer shown here is a net-neutral polyampholyte. For polyelectrolytes, counterions will also be present. The picture is produced with GISMOS.⁴⁶

of a fixed length b . The electrostatic term is

$$U_{\text{el}} = \sum_{i < j}^{N + N_c} \frac{q_i q_j e^2}{4\pi\epsilon_r \epsilon_0 |\mathbf{r}_i - \mathbf{r}_j|} \quad (3)$$

where q_i is the valence of particle i and e is the elementary charge. U_{hc} is a hard core potential given by

$$U_{\text{hc}} = \begin{cases} 0, & |\mathbf{r}_i - \mathbf{r}_j| \geq d \\ \infty, & |\mathbf{r}_i - \mathbf{r}_j| < d \end{cases} \quad (4)$$

In the simulations reported here, the following parameters are used: $d = 4 \text{ \AA}$, $K = 14 \times 10^{-3} \text{ N/m}$ or $b = 6 \text{ \AA}$ and $\epsilon = 78$ (the value for water at $T = 298 \text{ K}$). The above values have been frequently used in simulations, and the behavior of such chains are thus well characterized. The force constant is chosen so that, when no external stress or strain is applied, the uncharged polymers with Gaussian bonds will have the same mean bond length r_{mm} as the fixed bond length b . For the PAs, all monomers have a valence of either $q_m = +1$ or -1 and the net charge of the chain is zero. Both block PAs, with a block size n , and random PAs are considered. For the PEs, the monomers have a valence of $q_m = +1$ and the counterions can have a valence $q_c = -1, -2, -3, \text{ or } -4$ and obeys the electroneutrality condition

$$Nq_m + N_c q_c = 0 \quad (5)$$

All simulations are carried out in three dimensions except the special case corresponding to Figure 8 which is a one-dimensional calculation.

2.2. Stress Ensemble. For simulations in the stress ensemble, an external force F is applied at the two ends of the polymer, and force-extension curves are constructed by plotting the force against the equilibrium root-mean-square end-to-end distance $\sqrt{\langle R_{\text{EE}}^2 \rangle}$, shortened to simply R_{EE} . The Hamiltonian, including the effect of the external force, is given by

$$U_{\text{tot}} = U_0 - Fz_N \quad (6)$$

where z_N is the coordinate, in the direction of the applied force, of the last monomer with the origin located at the first monomer. A schematic figure of the systems is showed in Figure 1.

Simulations in the stress ensemble are performed with both zero and one wall. In the case without walls, the chain and counterions are enclosed in a spherical cell, whereas in the case

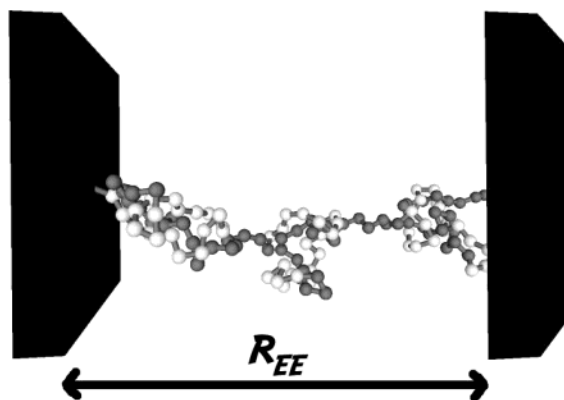


Figure 2. Schematic figure of the model used in the strain ensemble. The different charges are distinguished by the two shades of gray and the polymer shown here is a net-neutral polyampholyte. The picture is produced with GISMOS.⁴⁶

with one wall, half the cell is closed off for the particles resulting in a cell with the shape of a hemisphere.

The cell model is well suited for studying single polymer properties.²⁸ Every cell contains one polymer chain and counterions. If required, salt can also be added while maintaining electroneutrality in the cell.

Simulations are carried out in the canonical ensemble in which monomers are moved by simple translations and/or with a pivot move and the small ions are translated. Energies are computed from eq 6 and moves are accepted according to the Metropolis MC scheme.^{29,30} The autocorrelation for the end-to-end distance R_{EE} has been measured and the simulations are run over at least a few hundred independent configurations to ensure good statistics.

2.3. Strain Ensemble. In the strain ensemble, the end-to-end distance R_{EE} is imposed as a constraint and the resulting average force F is measured at equilibrium. In this case, the Hamiltonian is

$$U_{\text{tot}} = U_0 \quad (7)$$

Simulations in the strain ensemble are performed with two walls present. A schematic figure of the system is showed in Figure 2. Only PAs and neutral polymers are studied with this system.

The lateral force will be equal across the system, and for numerical reasons, the force, due to the polymer, is calculated at the midplane^{31–33} as

$$F = F_{\text{el}} + F_{\text{kin}} + F_{\text{bridge}} + F_{\text{coll}} \quad (8)$$

where the electrostatic correlation force F_{el} is due to the sum of direct Coulombic interaction between charges on one side of the mid-plane and charges on the other side. F_{kin} is the kinetic force due to collisions with the (imaginary) midplane and is related to the local concentration of the different particles, $F_{\text{kin}}/\text{unit area} = kT \sum \rho_i$ (midplane), where ρ_i is the concentration of particle type i . The bridging term F_{bridge} is the lateral component of the force due to polymer bonds crossing the midplane, and the last term F_{coll} is given by hard sphere collisions between particles at the midplane.

Simulations are carried out in the canonical ensemble in which monomers are moved by simple translations. Energies are computed from eq 7 and moves are accepted according to the Metropolis MC scheme.^{29,30} The autocorrelation for the force has been measured, and the simulations are run over at least a few hundred independent configurations to ensure good statistics.

2.4. Free Energy Method. To construct a force-extension curve using the stress or strain ensemble, each point of the curve requires a separate simulation. An alternative method is to modify the MC procedure with a suitable penalty function U^* so that all end-to-end distances (and forces) are equally probable. The method presented here resembles umbrella sampling but is different in that the penalty function is not given as an input to the simulation but is generated during the simulation. This penalty function turns out to be related to the potential of mean force (PMF), $w(R_{EE})$, between the two ends of the chain.^{34,35} The force-extension curve is the derivative of $w(R_{EE})$ with respect to R_{EE} .

A straightforward way of calculating the PMF, in a normal simulation, is to simply calculate the probability of finding the system at a certain end-to-end distance $p(R_{EE})$ because the PMF is connected to the probability by

$$w(R_{EE}) = -k_B T \ln p(R_{EE}) \quad (9)$$

where k_B is the Boltzmann constant and T is the temperature. However, because the probability of visiting high energy states is low, configurations far from the average R_{EE} , i.e., the extended or compressed configurations, will be sampled infrequently if at all during a simulation. However, by adding an appropriate penalty function U^* to the normal, undisturbed, MC Hamiltonian of eq 1, it is possible to sample all states of interest.

In the canonical ensemble, the probability distribution along any reaction coordinate ζ is given by

$$p(\zeta_0) = \frac{\int \exp[-\beta U(\mathbf{r})] \delta[\zeta - \zeta_0] \mathbf{dr}}{\int \exp[-\beta U(\mathbf{r})] \mathbf{dr}} \quad (10)$$

where \mathbf{r} represents all particle coordinates and $\beta = 1/k_B T$. Adding the penalty function results in a modified probability distribution

$$p^*(\zeta_0) = \frac{\int \exp[-\beta \{U(\mathbf{r}) + U^*(\zeta_0)\}] \delta[\zeta - \zeta_0] \mathbf{dr}}{\int \exp[-\beta \{U(\mathbf{r}) + U^*(\zeta_0)\}] \mathbf{dr}} \quad (11)$$

The original probability distribution can be retrieved from

$$p(\zeta) = C_1 p^*(\zeta) \exp[\beta U^*(\zeta)] \quad (12)$$

where C_1 is a constant. If a simulation is run with a penalty function resulting in a constant $p^*(\zeta)$ this will give

$$p(\zeta) = C_2 \exp[\beta U^*(\zeta)] \quad (13)$$

where C_2 is another constant. Identifying with eq 9, it is clear that

$$U^*(R_{EE}) = -w(R_{EE}) + C_3 \quad (14)$$

where C_3 is a physically unimportant constant, because we are interested in the derivative of w or U^* , which is the force-extension curve.

The problem is now to construct U^* that will give rise to a uniform distribution of end-to-end distances. The penalty function $U^*(R_{EE})$ is discretized over R_{EE} into equal size intervals. At the start of the simulation, the penalty function U^* is taken to be uniform. Every time the end-to-end distance falls within a particular interval of R_{EE} , the corresponding U^* is increased by a certain value δU^* . This ensures that the distribution function $p^* \sim \exp[-\beta(U + U^*)]$ will approach a constant.

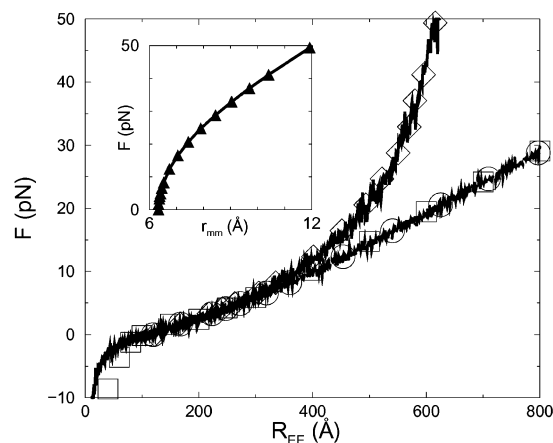


Figure 3. Force-extension curves for neutral polymers with $N = 120$ obtained using the different methods described in the text are used. Polymers with Gaussian bonds are simulated with applied stress (circles), with applied strain (squares), and with the free energy method (bottom solid line). Polymers with a fixed bond length are simulated with applied stress (diamonds) and with the free energy method (top solid line). The inset shows how the size of the Gaussian bonds r_{nm} grows with increasing imposed force.

A technical problem is that keeping δU^* constant during the full extent of the simulation will lead to poor statistics. The difference in energy before and after a MC move will be calculated as $\Delta U + \delta U^*$. When the distribution function becomes uniform, U^* will start to be updated equally over all R_{EE} , and the fluctuations in δU^* will start to dominate and obscure the information in ΔU . This problem is circumvented by decreasing the penalty as the simulation progresses.³⁴ In this paper, the choice for δU^* is $0.1k_B T$ at the beginning of the simulation. This is then updated by $\delta U^*_{new} = \delta U^* / \text{MIN}[U^*(R_{EE})]$, where $\text{MIN}[U^*(R_{EE})]$ is the minimum value of U^* found for the different discretized values of R_{EE} .

Each simulation is run until $p^*(R_{EE})$ is verified to be uniform which guarantees good results for the PMF.

3. Uncharged Polymers

The only interactions present for the neutral polymers are the hard sphere repulsions and the nearest monomer bond interactions, which is the model known as the self-avoiding walk (SAW). In Figure 3, force-extension curves for polymers with $N = 120$ are shown. For the chain with Gaussian bonds, all three methods presented in section 2 are used. For the stress method, no walls are present, and for the strain method, two walls are present, and the free energy method has one wall. Independent of the choice of method or the number of walls, the same results are obtained for undisturbed and for stretched polymers, i.e., for $F \geq 0$. When the polymer is compressed ($F < 0$), the presence of two constraining walls results in a larger negative force, because the configurational space is smaller for the polymer.^{36,37}

The polymers with fixed bond length have been simulated within the stress ensemble and with the free energy method. Again the results agree. The curves for the polymers with a fixed bond length follow the curves of the polymers with Gaussian bonds up until about $F = 6$ pN. This range of extension is sometimes called entropic stretching because the mean bond length of the polymer with Gaussian bonds does not change. This can also be observed in the insert of Figure 3 which shows that the bond length for the polymers with Gaussian bonds is constant for small forces. When the force increases further, the bond length then increases. Because of

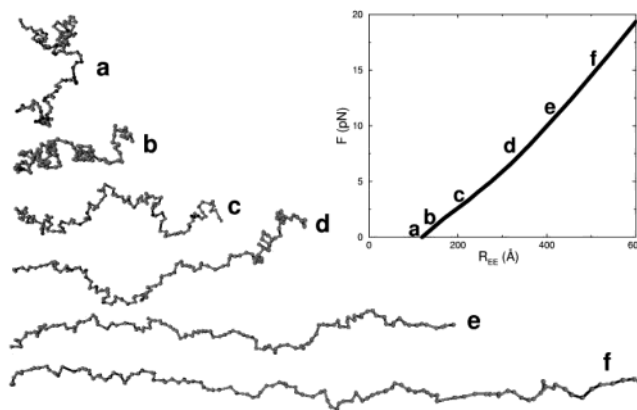


Figure 4. Snapshots from MC simulations of a neutral polymer in the stress ensemble. The polymer has Gaussian bonds and the number of monomers is $N = 120$. From top to bottom, the external force is (a) $F = 0$, (b) $F = 1.6$, (c) $F = 4$, (d) $F = 8$, (e) $F = 12$, and (f) $F = 16$ pN. The inserted diagram points out where in the force-extension curve the snapshots are taken.

the nature of the bond potential, the bond length and the end-to-end distance will increase linearly with the force. Stretching of the polymer due to stretching of the bonds is sometimes referred to as enthalpic stretching. Obviously, the polymers with a fixed bond length cannot expand in the same way, and when the entropic stretching has been exhausted, the force increases rapidly with extension.

The crossover to this so-called finite extensibility regime seems to take place between $2R_0$ and $3R_0$, where R_0 is the undisturbed R_{EE} , i.e., at $F = 0$, which is in agreement with earlier observations.³⁸ In most single molecule experiments performed, it is actually this regime that is probed,²¹ which is a reason to why many different molecules can be fitted to simple polymer models such as the WLC and FJC.

A more realistic polymer will have features from both the model with extensible bonds and the model with fixed bonds. The bonds will be able to stretch, but only to a certain limit, where the force will start to increase rapidly and eventually even break the bonds.

Simulation snapshots of uncharged polymers, corresponding to various applied forces, are shown in Figure 4. For small forces, it is clear that the polymer is unfolding (entropic stretching), whereas at higher force, the polymer is almost linear and the only way of stretching the polymer further is by stretching the individual bonds (enthalpic stretching).

4. Polyampholytes

In addition to the monomer–monomer hard sphere interactions and bond laws of the uncharged polymers, each monomer of polyampholytes carries a charge. Although experimentally realizable polyampholytes often have neutral monomers, in simulations, it is convenient to let all monomers have either a positive or negative charge. This allows for a more effective assessment of the electrostatic effects given the limited chain length that can be considered in simulations.

Net-neutral PAs are either characterized by random charge distributions or by a repeating sequence of n positive and n negative monomers. Because of electrostatic interactions, both random and block-PAs generally collapse for all but the smallest block sizes.³⁹ This compaction is sometimes called the polyampholyte effect. If the PA has a net charge, the polyelectrolyte effect will come into effect trying to unfold the chain. The configuration of the PA will depend on a complicated balance between the attractive and repulsive electrostatic forces.^{7,9,11–13,15,40}

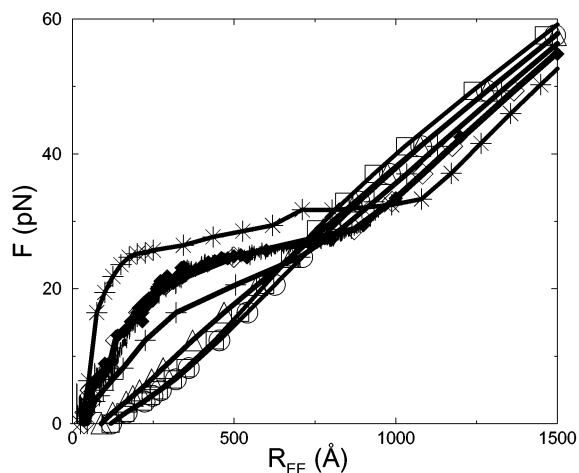


Figure 5. Force-extension curves for block-polyampholytes with $N = 120$ and block size $n = 1$ (squares), $n = 4$ (triangles), $n = 10$ (pluses), $n = 20$ (diamonds), $n = 60$ (stars), and an uncharged polymer (circles). All simulations are performed with an applied stress (open symbols and connected by the solid line) except for the $n = 20$ case which also is simulated with applied strain (filled diamonds) and with the free energy method (solid thin fluctuating line).

Between the two extreme cases of a collapsed net-neutral PA and an extended polymer where the PE effects dominate, there is a possibility of the chain forming so-called pearl-necklace structures.

Pearl-necklace structures have been predicted theoretically for PAs, where pearl-necklaces will form as a competition between the PA effect and the PE effect.^{12,23} Also hydrophobic PEs are thought to form pearl-necklaces as a competition between the expanding PE effect and the compacting hydrophobic interactions.⁴¹

Although these electrostatically induced pearl-necklace structures have been observed in simulations^{15,42,43} their existence has not been confirmed by experimental observations. The effects of the competing electrostatic interactions will be manifest in the force-extension curves of the charged polymer and thus provide a feasible way to extract information for these systems.

In this section, the polyampholyte effect together with an externally applied force will be studied in detail; thus, only net-neutral PAs will be discussed. The polyelectrolyte effect is deferred to section 5.

Force-extension curves for block-polyampholytes with different block sizes are shown in Figure 5. At $F = 0$, it is obvious that the chains with small block sizes have the same R_{EE} as the uncharged chain and that chains with bigger block sizes have smaller values of R_{EE} . With increasing F , the force-extension curve for the alternating chain ($n = 1$) follows that of the uncharged polymer. As the block size increases, the stretching behavior deviates from that of an uncharged chain. For the PAs with $n = 20$ and 60 , a plateaulike region is found in which the force does not change substantially for a wide range of the end-to-end distances.

It has been put forward that pearl-necklace forming polymers would give rise to a plateau in the force-extension curve and that this constant force regime would be due to the unfolding of the pearls.^{22,44} Snapshots of the unfolding PAs, Figure 6, show how the different block-PAs unfold.

For $n = 4$, the snapshots closely resemble those of the neutral polymer shown in Figure 4. For small forces, the chains are not very compact, and for increasing forces, both chains unfold in a regular fashion. Only at $F = 8$ pN (snapshot c) is there a

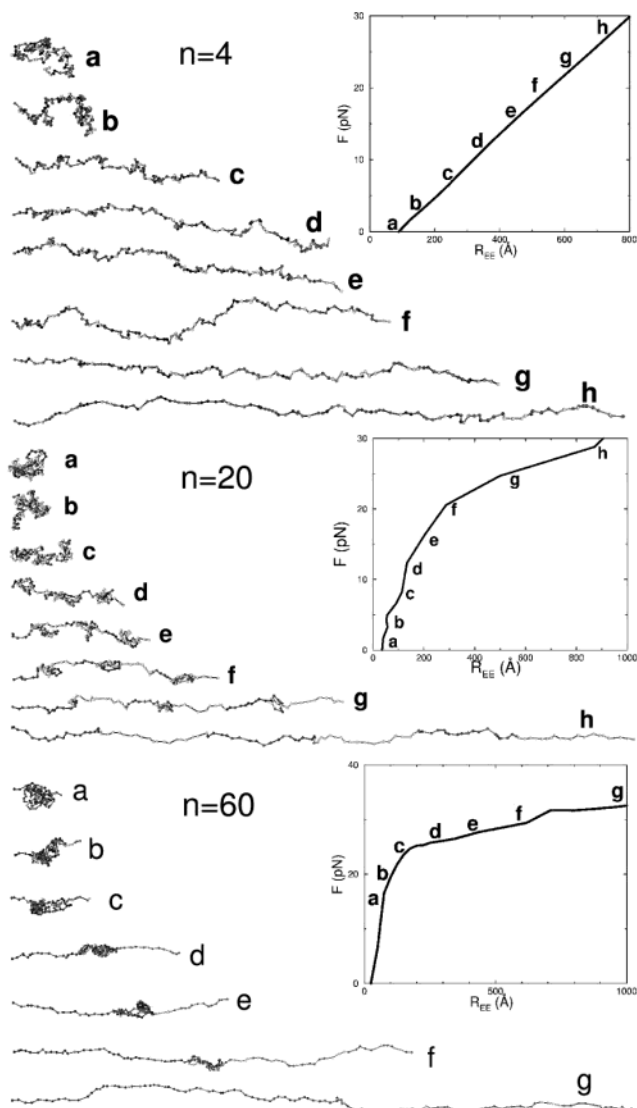


Figure 6. Snapshots from MC simulations of block-polyampholytes with a block size of $n = 4$ (top), $n = 20$ (middle), and $n = 60$ (bottom). The number of monomers are $N = 120$ and Gaussian bonds are used. The snapshots are taken from simulations with an external force. The inserted diagrams point out where in the force-extension curve the snapshots are taken. For the $n = 4$ case, the following forces are applied: (a) $F = 0$, (b) $F = 4$, (c) $F = 8$, (d) $F = 12$, (e) $F = 16$, (f) $F = 20$, (g) $F = 24$, and (h) $F = 28$ pN. For the $n = 20$ case, the following forces are applied: (a) $F = 0$, (b) $F = 4$, (c) $F = 8$, (d) $F = 12$, (e) $F = 16$, (f) $F = 20$, (g) $F = 24$, and (h) $F = 28$ pN. For the $n = 60$ case, the following forces are applied: (a) $F = 16$, (b) $F = 20$, (c) $F = 24$, (d) $F = 26$, (e) $F = 27.5$, (f) $F = 29$, and (g) $F = 33$ pN. The snapshots are produced with GISMOS.⁴⁶

possible resemblance of pearl-necklace structures. Within this particular polymer model, grouping the charges in blocks of four is not enough to induce compaction and counteract the external pulling force.

Turning to the $n = 20$ case, the PA is compact for small forces. Increasing the force slightly distorts the shape of the chain, elongating it in the force direction into a more cylindrical form. For stronger forces, the chain forms three separate pearls. These are formed in the junctions between the positive and negative charges, but interestingly enough, pearls do not form at all of the five junctions. For forces where pearls are observed, the force-extension curve flattens out, although it does not form a totally flat plateau. A similar behavior has been observed in simulations of hydrophobic polyelectrolytes forming pearl-

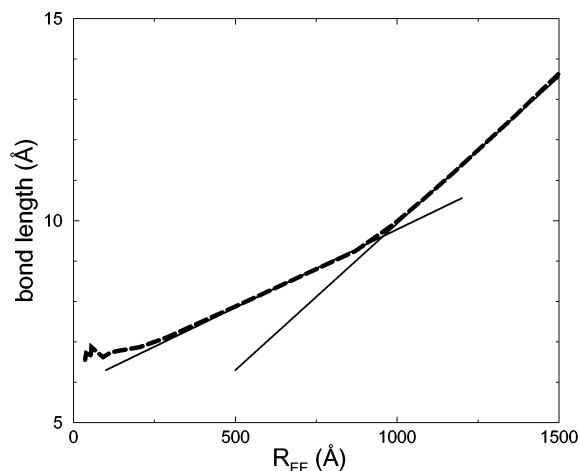


Figure 7. Variation of the bond length as the PA ($N = 120$, $n = 20$) unfolds is shown by the thick dashed line. The thin solid lines are just guides to point out different regimes.

necklace structures,⁴⁵ and the underlying mechanism is attributed to thermal fluctuations in the number of pearls.⁴⁴ Although this should show up in all equilibrium simulations as well as experiments, sometimes the pulling of the polymer is performed at a speed that does not allow full equilibrium, and thus, the plateau may be more pronounced.

The di-block case, $n = 60$, is an extreme of the pearl-necklace forming PA. The polymer stays compact up to high forces, where it starts to elongate. At a certain force, the ends of the polymer starts to leave the still compact center. This is when the plateau phase is reached in the force-extension curve. The force is more or less constant until all of the monomers have left the single pearl.

Force-extension curves obtained with the three different methods described in section 2 are shown for the pearl-necklace forming, $N = 120$, $n = 20$, block-PA in Figure 5. Just as for the uncharged polymer, the results are identical within statistical limits except at small applied forces which can be attributed to the presence of the different number of walls.

The length of the Gaussian bonds for the pearl-necklace forming polymer, $N = 120$, $n = 20$, as it is being stretched, is shown in Figure 7. For small external forces, the bond length does not change much, in what could be seen as an equivalent to the entropic stretching for neutral polymers. For larger forces, two different stretching regimes occur for the bonds: one in which the pearls are present and one when all the monomers are pulled out of the pearls. The expansion of the bond is larger in the latter regime. One reason as to why the plateaus seen in Figure 5 are not totally flat is that the bond length increases even when the polymer is in the plateau. Thus, a complicated balance of stretching single bonds in the necklace and unpacking the electrostatically compacted pearl is maintained. The flatness of the plateau would depend on this balance and, for example, PAs with a fixed bond length do not show a pronounced plateau.

For highly stretched PAs ($R_{EE} > 800$ Å), it is shown in Figure 5 that a smaller force is required to stretch a PA with high n than an uncharged polymer. This is opposite to the behavior at moderate forces, where the force needed to stretch a PA to a given length increases with increasing block size. To elucidate this force-extension behavior observed for PAs with highly stretched structures, polymer configurations, in which the monomers are constrained to lie sequentially on a straight line, are studied. The results of stress ensemble simulations in which the monomers can only move in one dimension along a straight

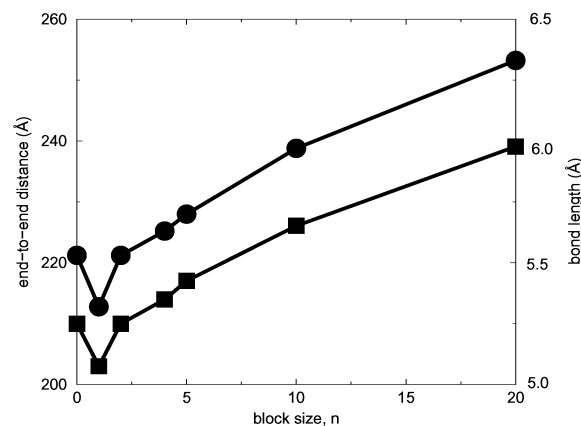


Figure 8. Variation of the end-to-end distance (squares) and the bond length (circles) for different block sizes for a polyampholyte constrained to one dimension. $n = 0$ corresponds to the uncharged polymer. The chain size is $N = 40$ and Gaussian bonds have been used.

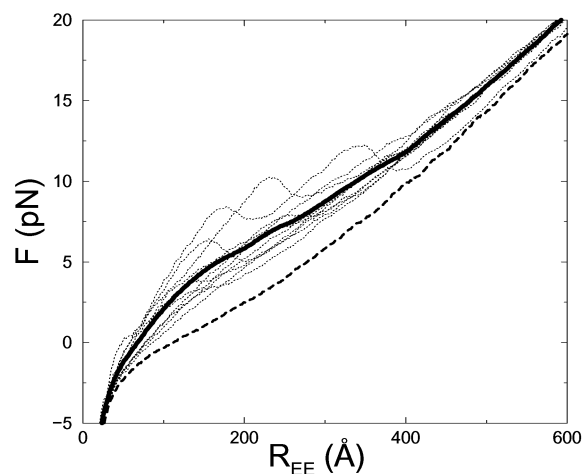


Figure 9. Force-extension curves for 10 different random polyampholytes with $N = 120$ and Gaussian bonds (dotted lines). Also shown is the averages of all 10 (solid line) and the corresponding uncharged polymer (dashed line). The free energy method is used to obtain the curves, and the fluctuations are filtered out by using running averages.

line are shown in Figure 8. The mean bond length and end-to-end distance for PAs with Gaussian bonds are shown as a function of block size. In contrast to the behavior of PAs in three dimensions, increasing block size actually increases the chain size. Only the $n = 1$ PA is smaller than the uncharged polymer. This is in agreement with observations at large R_{EE} in Figure 5, where only the $n = 1$ curve lies above that of the uncharged chain. The crossover in the force-extension curves of charged PAs and the uncharged polymer at large R_{EE} indicates that in highly stretched conformations the PAs electrostatic interactions act to expand the PA rather than provide a compacting force.

Turning to random PAs, the extra complexity of different charge sequences is added. In Figure 9, the results for 10 different sequences are shown. Although the different charge realizations have the same average block length of about two, as any random PA with large enough N , they have distinctly different behavior. Some curves show specific structure before they fall into the curve of an uncharged polymer, whereas others follow that curve closely.

When examining snapshots of the random charge sequences, it is possible to find pearl-necklace structures as seen in Figure 10 although they do not seem to be the dominating structure.

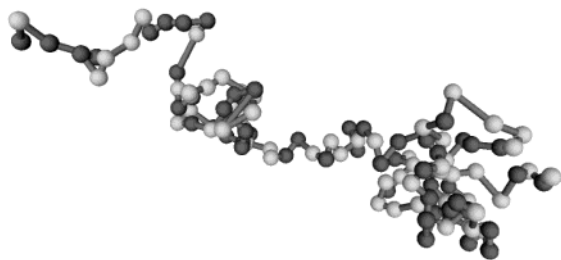


Figure 10. Snapshot from a MC simulations of a random polyampholyte showing a pearl-necklace like configuration. The number of monomers are $N = 120$ and Gaussian bonds are used. For this configuration $R_{EE} = 120 \text{ \AA}$. The snapshots are produced with GIS-MOS.⁴⁶

Also the length of the PAs investigated here could be too small for the formation of pearl-necklace structures.

5. Polyelectrolytes

Turning to polyelectrolytes, where counterions have to be added to the system to keep it electroneutral, the valance of the counterions is important, and it has been shown that the presence of multivalent counterions can collapse flexible polyelectrolytes.^{5,6} In Figure 11, the force-extension curves of PEs with different counterions are shown. For no applied force, it is clear how a counterion valance of $q_c = 3$ compacts the PE to about the same size as the uncharged polymer and the $q_c = 4$ induces an even smaller size. For $q_c = 1$ and 2, the PEs are much more extended than for the uncharged chain. Also, the polymers with Gaussian bonds are more extended than their counterparts with fixed bond length, implying that the bonds are stretched even for $F = 0$.

When applying an external force, the PEs compacted by multivalent counterions expands more than the PE with monovalent counterions which is already expanded due to monomer–monomer repulsion. Thus, for the case of a highly charged PE with monovalent counterions, only the finite extensibility regime will be explored as seen in Figure 11a.

Although the force-extension curves for PEs with different counterions are quantitatively different, as shown in Figure 11, they all have similar shapes as the curve for the uncharged polymer in contrast to the PA force-extension curves in Figures 5 and 9. Thus, although both PAs and PEs with multivalent counterions are compacted due to electrostatics, their response to external forces are markedly different. The compacting forces of a PA is larger than the compacting forces of a PE with multivalent counterions which should reflect on the chain conformations. This behavior can be quantified by considering the end-to-end distribution functions, plotted in Figure 12.

For the uncharged polymer, the shape of the end-to-end distribution functions are almost independent of the applied force. For larger forces, the distributions are slightly sharper, indicating that stretching the polymer limits the conformations available for the polymer. For a polymer with fixed bond size, this will be even more evident as the extreme case of a fully stretched polymer only has one possible conformation.

The end-to-end distribution function for polyelectrolytes compacted by trivalent counterions is similar to that for the uncharged polymer, whereas the pearl-necklace forming block-polyampholyte behaves differently. For the compact PA, at zero applied force, the distribution function is narrow. Increasing the applied force opens up the PA and increases the fluctuations in the end-to-end distance. The width of the PA end-to-end distribution function reaches a maximum at the plateau ($F = 24 \text{ pN}$) in which the chain forms pearl-necklace structures. When

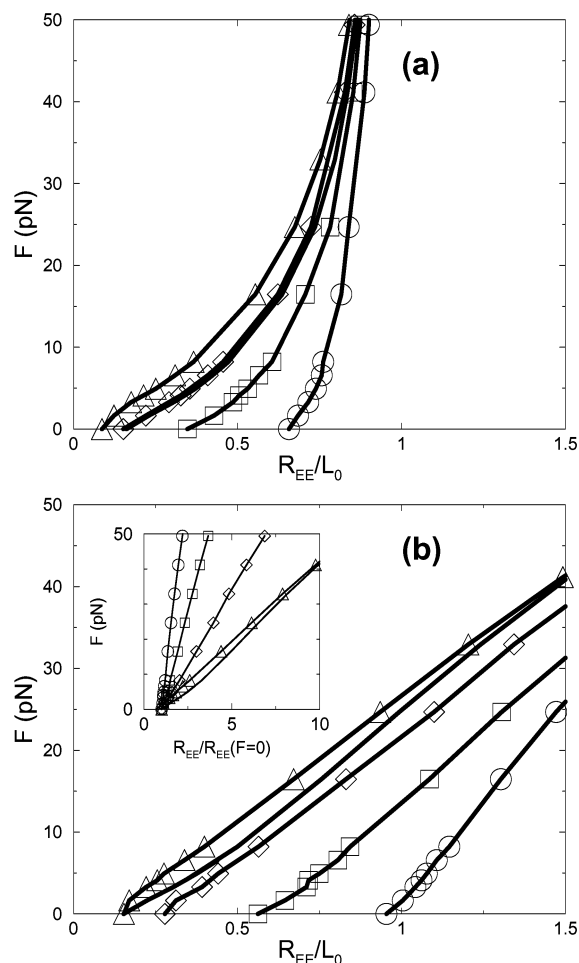


Figure 11. Force-extension curves for polyelectrolytes with (a) fixed bond sizes, $b = 6 \text{ \AA}$ and (b) Gaussian bonds. $N = 132$ and the counterion valance is $q_c = 1$ (circles), $q_c = 2$ (squares), $q_c = 3$ (diamonds), and $q_c = 4$ (triangles). Also shown is the uncharged chain (no symbol). On the x axis, the end-to-end distance is divided by L_0 , the contour length of the chain with a fixed bond size. In the inset of (b), the x axis is rescaled with the $F = 0$ end-to-end distance. In (a), the curves for $q_c = 3$ and the uncharged chain are on top of each other and cannot be distinguished.

applying an even larger force, the distribution becomes more narrow again as the PA becomes fully extended.

Thus, PAs resist external forces, forming exotic structures, better than flexible polyelectrolytes with multivalent counterions, which more or less follows the behavior of a SAW.

6. Conclusions

The three different models for simulating the force-extension curves of polymers can be used interchangeably for the systems studied here. For small applied forces, the influence of different kinds of geometrical constraints will be noticeable but do not greatly influence the response of the system subjected to an extension force. Simulations using the free energy method is the easiest to implement and also gives the full force-extension curve in one simulation.

When an external strain or stress is applied to a uncharged polymer, the monomers simply rearrange under small forces or extensions (entropic stretching). For larger forces, individual bonds are stretched (enthalpic stretching) until the finite extensibility regime is reached, where the polymer cannot stretch further and the force increases rapidly.

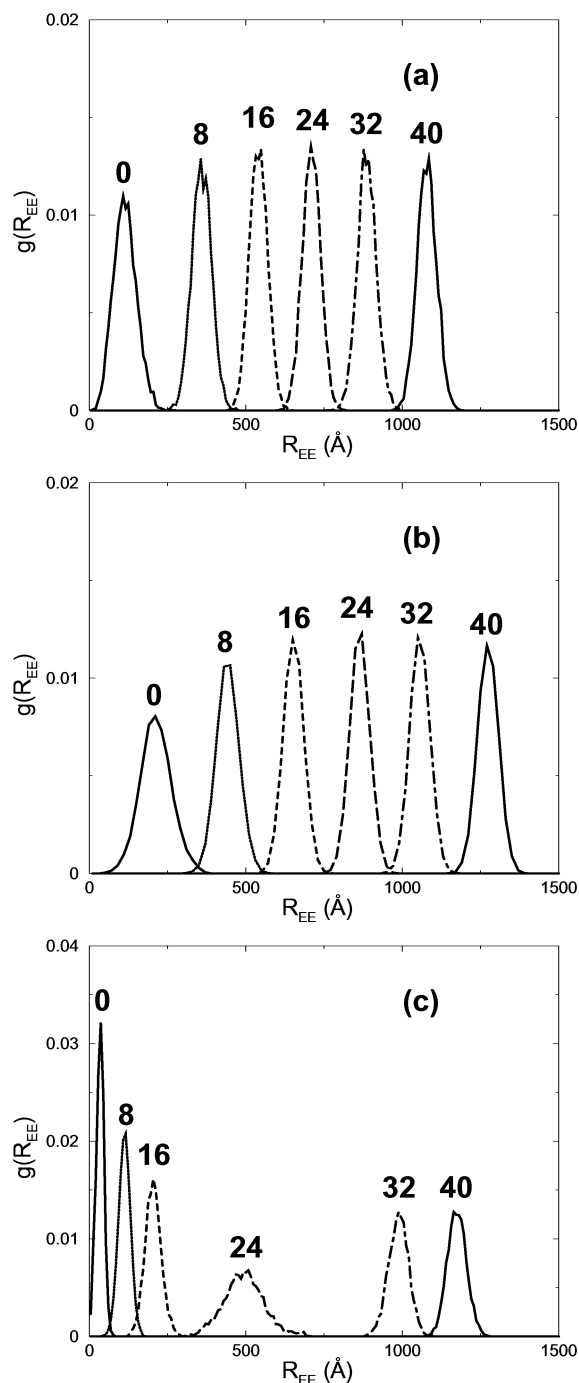


Figure 12. End-to-end distribution for (a) an uncharged polymer ($N = 120$), (b) a polyelectrolyte with trivalent counterions ($N = 120$, $q_c = 3$), and (c) a block-polyampholyte ($N = 120$, $n = 20$) at different applied forces. The curves are labeled with the applied forces in pN. Gaussian bonds are used.

Highly charged PEs with monovalent counterions are already stretched in comparison with the uncharged polymer. Further stretching will mostly probe the finite extensibility regime. When multivalent counterions, with a valance of three or larger, are present, the undisturbed PE is compacted. This compact PE behaves largely as an uncharged polymer when an external strain or stress is applied.

In the absence of an imposed stress or strain, net-neutral block-PAs form compact structures if the block size is large enough. They effectively resist unfolding when subjected to applied external strain or stress. In the plateau like regime in

the force-extension curve, exotic pearl-necklace structures are formed. Random PAs do not replicate this behavior, and although some pearl-necklace like conformations can be found, they are not the dominating structure.

Acknowledgment. We acknowledge Andrei Broukhno and Bo Jönsson for discussions regarding the free energy method. This work was in part supported by the Particulate Fluid Processing Centre, a special Research Centre of the Australian Research Council, the Victorian Partnership for Advanced Computing, and the Wenner-Gren Foundations.

References and Notes

- (1) Fujita, H. *Polymer Solutions*; Elsevier: Amsterdam, 1990.
- (2) Grosberg, A. Y.; Khokhlov, A. R. *Statistical Physics of Macromolecules*; AIP Press: New York, 1994.
- (3) Ullner, M. Polyelectrolyte models in theory and simulation. In *Handbook of Polyelectrolytes and their Applications*; Tripathy, S., Kumar, J., Halwa, H. S., Eds.; American Science: Los Angeles, CA, 2002.
- (4) Stevens, M. J.; Kremer, K. *J. Chem. Phys.* **1995**, *103*, 1669–1690.
- (5) Khan, M. O.; Jönsson, B. *Biopolymers* **1999**, *49*, 121–125.
- (6) Winkler, R. G.; Gold, M.; Reineker, P. *Phys. Rev. Lett.* **1998**, *80*, 3731–3734.
- (7) Ohlemacher, A.; Candau, F.; Munch, J. P.; Candau, J. *J. Polym. Sci., Polym. Phys. Ed.* **1996**, *34*, 2747–2757.
- (8) Kudaibergenov, S. E. *Adv. Pol. Sci.* **1999**, *144*, 115–197.
- (9) Higgs, P. G.; Orland, H. *J. Chem. Phys.* **1991**, *95*, 4506.
- (10) Wittmer, J.; Johner, A.; Joanny, J. F. *Europhys. Lett.* **1993**, *24*, 263–268.
- (11) Dobrynin, A. V.; Rubinstein, M. *J. Phys. II France* **1995**, *5*, 677–695.
- (12) Kantor, Y.; Kardar, M. *Phys. Rev. E* **1995**, *51*, 1299–1311.
- (13) Soddeman, T.; Schiessel, H.; Blumen, A. *Phys. Rev. E* **1998**, *57*, 2081–2089.
- (14) Tanaka, M.; Grosberg, A. Y.; Tanaka, T. *J. Chem. Phys.* **1999**, *110*, 8176–8188.
- (15) Yamakov, V.; Milchev, A.; Limbach, H. J.; Dünweg, B.; Everaers, R. *Phys. Rev. Lett.* **2000**, *85*, 4305–4308.
- (16) Perkins, T. T.; Quake, S. R.; Smith, D. E.; Chu, S. *Science* **1994**, *264*, 822–826.
- (17) Rief, M.; Gautel, M.; Oesterhelt, F.; Fernandez, J. M.; Gaub, H. E. *Science* **1997**, *276*, 1109–1112.
- (18) Mehta, A. D.; Rief, M.; Spudich, J. A.; Smith, D. A.; Simmons, R. M. *Science* **1999**, *283*, 1689–1695.
- (19) Haupt, B. J.; Senden, T. J.; Sevick, E. M. *Langmuir* **2002**, *18*, 2174–2182.
- (20) Baumann, C. G.; Bloomfield, V. A.; Smith, S. B.; Bustamante, C.; Wang, M. D.; Block, S. M. *Biophysical Journal* **2000**, *78*, 1965–1978.
- (21) Rief, M.; Gautel, M.; Oesterhelt, F.; Fernandez, J. M.; Gaub, H. E. *Science* **1997**, *276*, 1109–1112.
- (22) Halperin, A.; Zhulina, E. *Europhys. Lett.* **1991**, *15*, 417–421.
- (23) Kantor, Y.; Kardar, M. *Europhys. Lett.* **1994**, *27*, 643.
- (24) Wittkop, M.; Kreitmeier, S.; Göritz, D. *Phys. Rev. E* **1996**, *53*, 838–845.
- (25) Cifra, P.; Bleha, T. *Macromolecules* **1998**, *31*, 1358–1365.
- (26) Maurice, R. G.; Matthai, C. C. *Phys. Rev. E* **1999**, *60*, 3165–3169.
- (27) Kreitmeier, S.; Wittkop, M.; Göritz, D. *Phys. Rev. E* **1999**, *59*, 1982–1988.
- (28) Wennerström, H.; Jönsson, B.; Linse, P. *J. Chem. Phys.* **1982**, *76*, 4665.
- (29) Metropolis, N. A.; Rosenbluth, A. W.; Rosenbluth, M. N.; Teller, E.; Teller, E. *J. Chem. Phys.* **1953**, *21*, 1087–1097.
- (30) Allen, M. P.; Tildesley, D. J. *Computer Simulation of Liquids*; Oxford University Press: Oxford, 1989.
- (31) Guldbrand, L.; Jönsson, B.; Wennerström, H.; Linse, P. *J. Chem. Phys.* **1984**, *80*, 2221.
- (32) Valleau, J. P.; Ivkov, R.; Torrie, G. M. *J. Chem. Phys.* **1991**, *95*, 520.
- (33) Sjöström, L.; Åkesson, T.; Jönsson, B. *J. Chem. Phys.* **1993**, *99*, 4739.
- (34) Engkvist, O.; Karlström, G. *Chem. Phys.* **1996**, *213*, 63–76.
- (35) Kim, E. B.; Faller, R.; Yan, Q.; Abbott, N. L.; de Pablo, J. J. *Preprint, Cond. Mat* **2002**, 0208022.
- (36) Bright, J. N.; Stevens, M. J.; Hoh, J.; Woolf, T. B. *J. Chem. Phys.* **2001**, *115*, 4909–4918.
- (37) Pais, A. A. C. C.; Miguel, M. G.; Linse, P.; Lindman, B. *J. Chem. Phys.* **2002**, *117*, 1385–1394.

- (38) Titantah, J. T.; Pierleoni, C.; Ryckaert, J.-P. *Phys. Rev. E* **1999**, *60*, 7010–7021.
- (39) Khan, M. O.; Åkesson, T.; Jönsson, B. *J. Chem. Phys.* **2001**, *116*, 3917–3924.
- (40) Neyret, S.; Ouali, L.; Candau, F.; Pefferkorn, E. *J. Colloid Interface Sci.* **1995**, *176*, 86–94.
- (41) Dobrynin, A. V.; Rubinstein, M.; Obukhov, S. P. *Macromolecules* **1996**, *29*, 2974–2979.
- (42) Chodanowski, P.; Stoll, S. *J. Chem. Phys.* **1999**, *111*, 6069–6081.

- (43) Micka, U.; Holm, C.; Kremer, K. *Langmuir* **1999**, *15*, 4033–4044.
- (44) Vilgis, T. A.; Johner, A.; Joanny, J.-F. *Eur. Phys. J. E* **2000**, *2*, 289–300.
- (45) Limbach, H. J.; Holm, C.; Kremer, K. *Preprint, Cond. Mat.* **2002**, 0206274.
- (46) Lejdfors, C.; Khan, M. O.; Ynnerman, A.; Jönsson, B. *Lecture Notes of Comput. Sci. and Eng.* **2000**, *13*, 154–164. GISMOS is available for free download at <http://www.teokem.lu.se/gismos>.